Environ Biol Fish
DOI 10.1007/s10641-006-9124-2

SI-ELASMOBRANCHS

Elemental signatures in the vertebral cartilage of the round stingray, *Urobatis halleri*, from Seal Beach, California

Loraine F. Hale · John V. Dudgeon · Andrew Z. Mason · Christopher G. Lowe

Received: 6 June 2006 / Accepted: 14 July 2006

Abstract Although numerous studies have utilized elemental analysis techniques for age determination in bony fishes, little work has been conducted utilizing t'hese procedures to verify age assessments or temporal periodicity of growth band formation in elasmobranchs. The goal of this study was to determine the potential of laser ablation inductively coupled plasma-mass spectrometry (LA-ICP-MS) to provide information on the seasonal deposition of elements in the vertebrae of the round stingray collected from Seal Beach, California. Spatially resolved time scans for elements across the round stingray vertebrae showed peaks in calcium intensity that aligned with and corresponded to the number of seasonal growth bands identified using standard light microscopy. Higher signals of calcium were associated with the wide opaque bands while lower signals of calcium corresponded to the narrow translucent bands. While a close alignment between the numbers of calcium peaks and annual growth bands was observed in round stingray samples aged 5 years or younger, this relationship was less well defined in vertebral samples from round stingrays over 11 years old. To the best of our knowledge, this is the first study of its kind to utilize ICP-MS to verify age assessments and seasonal band formation in an elasmobranch. The results from this preliminary study indicate that LA-ICP-MS elemental analysis of the vertebral cartilage of the round stingray may have potential to independently verify optically derived age assessments and seasonal banding patterns in elasmobranch vertebrae.

Keywords Round stingray · Elemental composition · TOF-ICP-MS · Laser ablation

L. F. Hale · J. V. Dudgeon · A. Z. Mason · C. G. Lowe
Department of Biological Sciences, California State University Long Beach, 1250 Bellflower Blvd., Long Beach, CA 90840, USA

L. F. Hale (✉)
NOAA Fisheries Service, Southeast Fisheries Science Center, 3500 Delwood Beach Rd., Panama City, FL 32408, USA
e-mail: Loraine.Hale@noaa.gov

J. V. Dudgeon · A. Z. Mason
Institute for Integrated Research in Materials, Environments and Society, California State University Long Beach, 1250 Bellflower Blvd., Long Beach, CA 90840, USA

Introduction

Age and growth analyses are the first step in examining fundamental biological processes of a population of fish species (Casselman 1983). Estimations of the age structure of a population and growth rates of a species are used to determine

longevity, mortality, productivity, yield, and population dynamics which in turn are essential for management of populations (Casselman 1983). Ages are typically assessed by enumerating the growth bands in calcified structures such as the otoliths and vertebrae using light microscopy, which correlate closely with the age of the fish (Casselman 1983). While this approach is applicable for most bony fishes, it cannot always be utilized for some species such as elasmobranchs which do not have comparable calcified structures (Cailliet et al. 1986).

A number of alternative approaches have been advocated for determining age in cartilaginous fishes. The use of disequilibrium analyses between radioisotopes through bomb radiocarbon dating has provided a method for age validation for many hard-to-age fish such as rockfish (Kastelle et al. 2000; Cailliet et al. 2001; Andrews et al. 2005) and has been applied to elasmobranchs (Campana et al. 2002). Welden et al. (1987) used radiometric dating to determine ages of the leopard shark, *Triakis semifasciata*, the Pacific angel shark, *Squatina californica*, the common thresher shark, *Alopias vulpinas*, and the white shark, *Carcharodon carcharias*, but found that the age estimates based on radiometric dating were highly variable and in some cases predicted negative ages. However, Campana et al. (2002) subsequently utilized radiometric dating techniques to successfully age the porbeagle, *Lamna nasus*, and the shortfin mako shark, *Isurus oxyrinchus*.

Another more generally applicable approach that has been used to age elasmobranchs has been to utilize spatially resolved elemental analyses to determine the periodicity of annual growth bands in cartilaginous structures such as vertebrae. Energy dispersive X-ray microanalysis was used by Jones and Geen (1977) to determine the age of the spiny dogfish, *Squalus acanthias.* They found the peaks of calcium and phosphorus in the dorsal fin spine corresponded with age estimations from length–frequency analysis and suggested that elemental analysis of the cartilage of elasmobranchs could be useful in ageing elasmobranchs when no alternate ageing structure can be found (Jones and Geen 1977). Cailliet and Radtke (1987) used electron microprobe analysis to spatially analyze the temporal peaks in calcium and phosphorus in the vertebrae of the gray reef shark, *Carcharhinus amblyrhynchos*, and the common thresher shark, *Alopias vulpinus*, and found a strong correlation between the periodicity of deposition of these elements and optically determined annual growth band counts. They suggested the use of elemental analysis of elasmobranch vertebral cartilage as a way to verify the temporal periodicity of growth bands; however, no further studies have been published using this procedure for age verification in this group of fishes.

The current study aims to investigate the utility of laser ablation inductively coupled plasma mass spectroscopy (LA-ICP-MS) as a new methodology for studying the spatial distribution of elements in elasmobranch cartilage. The major advantage of LA-ICP-MS for studying the spatial distribution of elements in a solid sample over other established techniques such as energy dispersive (EDX) and wavelength dispersive X-ray (WDX) spectroscopy is its sensitivity. Thus, the relative elemental detection limits for interference free isotopes by LA-ICP-MS are generally in the sub-$\mu g\ g^{-1}$ range while those for EDX and WDX are typically in the 0.01–1% range (Campana et al. 1997; Durrant and Ward 2005).

The utility of this technique has been tested by identifying the seasonal and annual peaks in calcium and phosphorus in the vertebrae of the round stingray, *Urobatis halleri*, from Seal Beach, California and determining if these elemental peaks correspond with the annual periodicity of optically determined growth band pairs in the vertebrae. Recently, Hale (2005) utilized standard light microscopy to assess the calcified concentric growth bands in round stingray vertebral cartilage and determined that these fish live to be at least 14 years old and becomes sexually mature at 4 years of age. To the best of our knowledge, this is the first study of its kind to use elemental analysis by LA-ICP-MS for age assessment in an elasmobranch (Campana 2005).

Methods

Vertebrae preparation and ageing

Vertebrae were dissected from 12 specimens of round stingrays collected in 2003 and 2004

(Table 1). The vertebrae were mounted in Tap Plastics resin and a 0.5 mm wide bow-tie section was made using a Buehler isomet saw. Vertebral sections were viewed and growth bands were counted using a stereo-microscope with transmitted light field at 4× magnification (Olympus™ model SZX-12). Two readers independently assessed the age of each round stingray by counting the bands in individual vertebral centra. Annual periodicity of growth band formation was validated by maintaining 10 oxytetracycline-injected round stingrays in captivity for 2 years (Hale 2005).

Elemental composition

The round stingray vertebral sections were analyzed for elements using a GBC Optimass orthogonal time of flight inductively coupled plasma mass spectrometer (oTOF-ICP-MS) with an attached New Wave Research (Fremont, CA) LUV-213 high performance Nd:YAG UV laser operated at 213 nm (Reish and Mason 2003). Sectioned vertebrae samples were mounted on plexiglass slides and inserted into the ablation chamber of the laser system. Prior to analysis, the sections were pre-ablated with the laser to remove external contamination, after which the specimen chamber and transmission line was purged with high-purity argon gas to remove residual analytes in the sample introduction system. For data acquisition, a laser spot size of 30 μm with a constant energy density of 8.95 J $(cm^2)^{-1}$ and a repetition rate of 20 Hz was used to ablate the sample. The laser was scanned at a rate of 10 μm s^{-1} and elemental data was collected along a linear transect running through the focal region and from edge to edge of the whole vertebral corpus calcareum. The ICP-MS was operated in the time resolved mode. The instrumental conditions of operation were as follows: nebulizer flow 1.1 l min^{-1}; plasma flow 10 l min^{-1}; auxiliary flow 0.5 l min^{-1}; RF 1,600 W; skimmer –1,300 V; extraction lens –1,250 V; pushout plate 590 V; pushout grid –400 V; blanker 200 V; and reflectron 650 V. Calcium (^{44}Ca), phosphorus (^{31}P), magnesium (^{24}Mg) and strontium (^{88}Sr) were the main elements screened in the vertebral sections and the isotopic data were acquired at an acquisition rate of 1 point s^{-1}, representing a total ion pushout of 14,705.

Table 1 Round stingray samples used in ICP-MS elemental analysis. It is unknown when UH-094 was caught, so it was excluded from any seasonal analyses

Sample number	Sex	Disc width (mm)	Age (yr)	Month caught (mm/dd/yr)
19	M	250	11	05/16/03
54	M	82	0	10/24/03
69	F	151	5	08/15/03
74	F	253	12	09/19/03
86	F	104	1	01/30/04
94	F	95	1	–
100	F	143	5	03/19/04
105	M	84	0	03/19/04
114	M	150	3	05/19/04
116	F	155	4	06/09/04
149	F	154	4	08/27/04
159	M	254	12	08/27/04

Analytical precision was determined under these operating conditions for a suite of elements including sodium (Na), magnesium (Mg), aluminum (Al), silicon (Si), calcium (Ca), scandium (Sc), titanium (Ti), vanadium (V), chromium (Cr), manganese (Mn), iron (Fe), nickel (Ni), cobalt (Co), copper (Cu), zinc (Zn), arsenic (As), rubidium (Rb), strontium (Sr), yttrium (Y), zirconium (Zr), niobium (Nb), tin (Sn), antimony (Sb), cesium (Cs), barium (Ba), lanthanum (La), cerium (Ce), praseodymium (Pr), neodymium (Nd), samarium (Sm), europium (Eu), gadolinium (Gd), terbium (Tb), dysprosium (Dy), holmium (Ho), erbium (Er), thulium (Tm), ytterbium (Yb), lutetium (Lu), hafnium (Hf), tantalum (Ta), lead (Pb), thorium (Th), and uranium (U) using a NIST 612 glass standard reference material both before and after sample analyses (40 μg g^{-1}). The recorded %RSD values were typically below 6% over five analysis replicates with the exception of As and Zr which were 8.2 and 7.2%, respectively. Air analyses were used for blanks. Theoretical detection limits, based upon the 3σ value of the blank signal and the responses from the NIST 612, were typically <1 μg g^{-1} as reported by others (Sanborn and Telmer 2003; Trejos et al. 2002).

The presence of growth bands was determined from the peaks in the time resolved ion profiles and the spatial distribution of elemental

signatures was compared to the annual and seasonal periodicity of growth bands used for age assessment. Statistical tests to identify peaks from background noise were conducted using a statistical integration program (Origin™, Microcal Software Inc. 1997). An 11-point running average was applied to smooth the data, and peaks were identified using prescribed parameters within the software that included a minimum height of 3% of the total amplitude of the data in the range and a minimum width of 3% of the total number of points in the data range. For the elements of interest these values were approximate to the recommended 3σ of the smoothed blank signal (Sinclair et al. 1998; Sanborn and Telmer 2003).

Additionally, the spatial patterns in the ion intensity ratios of calcium to strontium, phosphorus and magnesium across the vertebrae were compared to identify changes in the relative distribution of these elements. Expression of the ion intensities in the form of ratios normalizes the ion intensities of the analytes to compensate for variations in laser ablation efficiency and topographical effects to provide a better index of the enrichment of these elements relative to ^{44}Ca along the transect (Reish and Mason 2003). Average Sr:Ca ratios were calculated by averaging the intensity ratio at each time point.

Results

A representative photomicrograph of a sectioned vertebrae across a transect, together with the corresponding smoothed spatial ion signal for ^{44}Ca, is shown in Fig. 1. Oscillations in the relative signal intensity of ^{44}Ca were observed along the transect that closely correlated with the identified growth bands with increased signal intensities occurring at the mid point of each yearly band and peaks in ^{44}Ca that were statistically identified above the background noise corresponded with growth bands (Fig. 1). Elevated signals were obtained from the edges of the specimen while a marked depression was noted in the ^{44}Ca signal at the foci of each vertebrae (Fig. 1). Analyses of other elements showed strong discernible signals for ^{88}Sr and ^{31}P that closely tracked the signal for ^{44}Ca (Fig. 2). Other

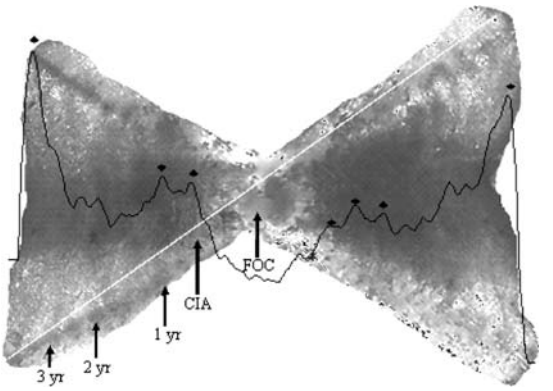

Fig. 1 Laser scan across a sectioned vertebrae of round stingray sample UH-114 showing the relative distribution of ^{44}Ca. The focus (FOC), change in angle (CIA), and year marks are indicated with arrows. The statistically determined peaks are indicated with a diamond (♦). The position of the laser transect is indicated with a diagonal line across the whole left corpus calcareum

elements producing pronounced signals correlating with ^{44}Ca included ^{24}Mg and ^{23}Na (not shown). Barium (^{137}Ba) was found primarily within the foci region while lead (^{208}Pb) was located at the edges of the vertebrae (not shown). No significant signals were obtained for other elements including uranium (^{238}U), niobium (^{93}Nb), and cerium (^{140}Ce) which have been recorded at relatively high concentrations within the biomineralized shells of various marine polychaetes (Reish and Mason 2003). Plots of the ion intensity ratios of ^{31}P and ^{24}Mg to ^{44}Ca showed that the relative abundances were conservative along the transect while those for ^{88}Sr showed

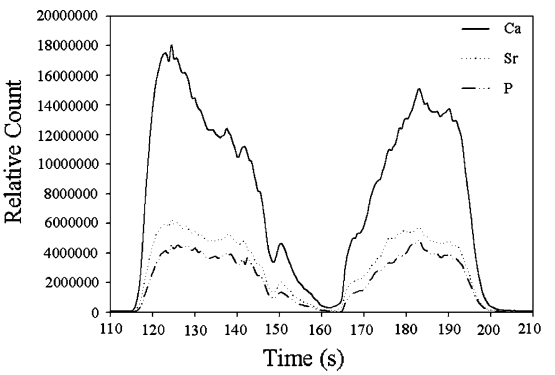

Fig. 2 Representative transect scan for calcium (^{44}Ca; solid line), strontium (^{88}Sr; dotted line), and phosphorus (^{31}P; dashed and dotted line) across a sectioned vertebrae of round stingray sample UH-054

variations in ratios indicative of differential deposition of these elements into the structure (paired t-test, $P = 0.004$; Fig. 3). The spatial periodicity of the changes in Sr:Ca ratio correlated with the growth bands and there was no significant difference in the statistically identified peaks between the ^{44}Ca time scan and the Sr:Ca ratio time scan (paired t-test, $P = 0.86$; Fig. 4). However, no discernable trends were observed between the mean Sr:Ca ion intensity ratio with age or date captured.

To determine whether the observed fluctuations in ^{44}Ca signal intensity within the cross sectioned vertebrae could be used to determine age, a series of analyses were conducted on different vertebrae samples from fish whose age was determined by counting the number of calcified growth bands using standard light microscopy (Hale 2005). Time resolved ion intensity profiles for ^{44}Ca for fish of age classes 0–1, 3–4, 5, and 11–12 showed an increase in the number of peaks ^{44}Ca in older aged fish (Fig. 5 a–d). However, the magnitude of the ^{44}Ca signal differed for samples of similar age (Fig. 5 a–d). Demarcations in the ^{44}Ca signal used to identify the tentative position of a growth band were determined visually in a manner comparable to that used optically to assess the age of the fish (Cailliet and Radtke 1987). There was a strong positive correlation between the number of ^{44}Ca peaks and the assessed age ($P < 0.001$, $r = 0.98$, Fig. 6).

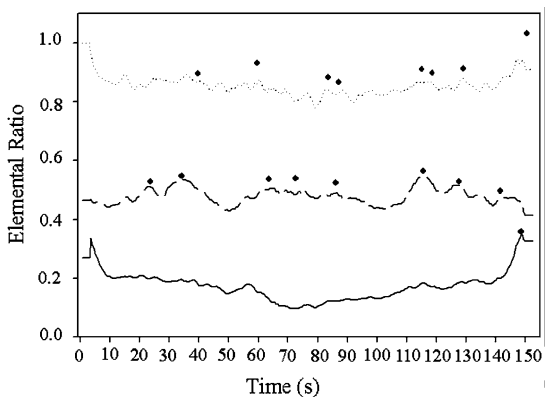

Fig. 3 Smoothed elemental ratios of ^{88}Sr (dashed line), ^{31}P (dotted line) and ^{24}Mg (solid line) normalized to the ^{44}Ca ion intensity across the vertebrae of round stingray sample UH-114. The statistically determined peaks are indicated with a diamond (♦)

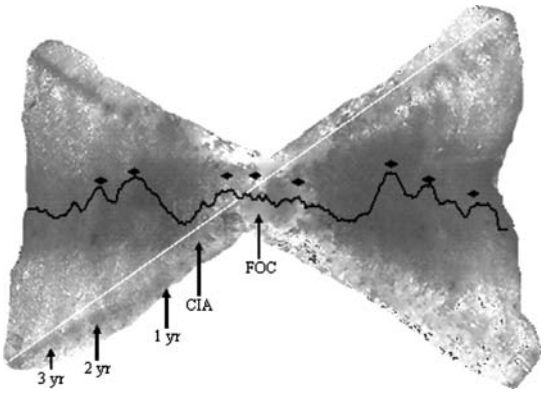

Fig. 4 Laser scan across a sectioned vertebrae of round stingray sample UH-114 showing the relative distribution of ^{88}Sr. The focus (FOC), change in angle (CIA), and year marks are indicated with arrows. The statistically determined peaks are indicated with a diamond (♦)

Discussion

Hale (2005) used centrum edge analysis to demonstrate that round stingrays expressed a pattern of seasonal growth in their vertebrae, with faster growth occurring in the summer months and slower growth occurring in the colder winter months. The observed patterns of peaks and valleys in ^{44}Ca correspond spatially with the seasonal growth bands, with higher peaks of ^{44}Ca corresponding to the wide opaque bands laid down in the summer months of warmer water and longer day lengths and lower valleys of ^{44}Ca corresponding to the narrow translucent bands deposited during the winter months of colder water and shorter day lengths. Cailliet and Radtke (1987) ascertained that the variation in calcium and phosphorus in the vertebrae of the grey reef shark and the common thresher shark was seasonal, with higher levels in the summer and lower levels in the winter. Similar patterns of seasonal deposition have been found using LA-ICP-MS in a bivalve, which had low strontium, magnesium, barium, and manganese levels in the winter and peaks in these elements in the summer (Leng and Pearce 1999).

The seasonal nature of the mineralization process produces a periodicity in the ^{44}Ca enriched bands that correlates closely with the assessed age of the fish. This correlative relationship is particularly strong in younger fish (up to age 5)

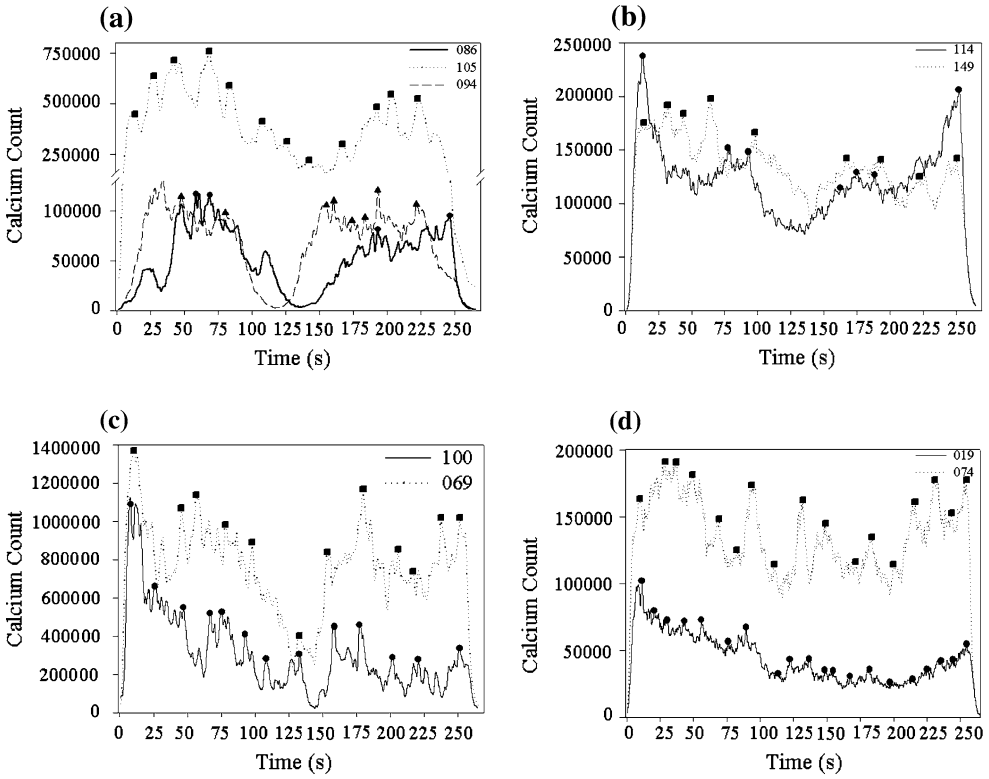

Fig. 5 (**a**) Transect scan for calcium for round stingray samples aged 0–1 year old. Statistically determined peaks are indicated with a symbol. (**b**) Transect scan for calcium for round stingrays aged 3–4 years old. Statistically determined peaks are indicated with a symbol. (**c**) Transect scan for calcium for round stingray samples aged 5 years old. Statistically determined peaks are indicated with a symbol. (**d**) Transect scan for calcium for round stingray samples aged 11–14 years old. Statistically determined peaks are indicated with a symbol

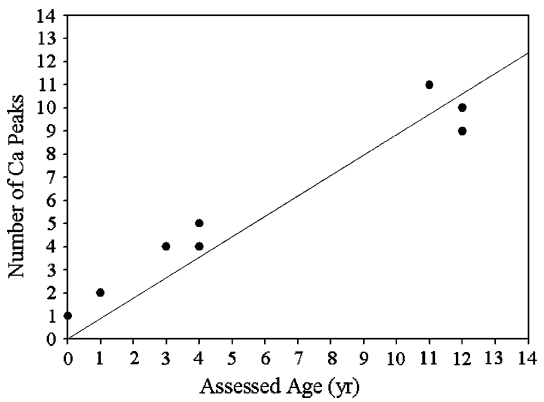

Fig. 6 Relationship between assessed age (yr) and number of calcium peaks in all samples from round stingrays ($P = 0.83$, $r = 0.98$)

where the bands are discrete and are sufficiently spatially resolved to enable the probe to ablate between the bands to give statistically definable depressions in the signals. However, this correlation is less defined in the older round stingrays, where the ICP-MS data show a tendency to underestimate the age of round stingrays over 11 years old. These findings are in accord with those of Panfili and Tomas (2001) who found that peaks in elements tended to underestimate the true age of tilapia in general, and that this underestimation was more pronounced in older fish.

One explanation for the discrepancy between the number of optically and analytically defined bands in older round stingrays is that in elasmobranchs the growth bands towards the perimeter of the vertebrae tend to become more closely opposed (Goldman 2004). Thus, light microscope estimations of the inter-band distances show a progressive decrease in distance with the age of the band with the 1–5 year old round stingray growth bands 95–160 μm apart while growth bands for 5–13 year old round stingrays were

44–66 μm apart (Hale unpublished data). Spatial resolution studies by Sanborn and Telmer (2003) on natural and artificially zoned materials have shown that the spatial resolution of LA-ICP-MS is influenced by a number of factors including spot size, scan rates, concentration gradients, memory effects and instrument acquisition parameters. Based on their data, it would appear that the distances between the outer bands of older stingrays are close to the expected attainable limit of spatial resolution using a LA-ICP-MS (Sanborn and Telmer 2003). If so, then a loss in signal amplitude below the statistical confidence window necessary for peak detection caused by signal overlap and averaging as the laser moves across adjacent bands would result in an underestimation in the numbers of bands in these older fish.

There was no discernable pattern in the relative amount of calcium present within the different annuli within a given vertebrae. Similarly, no trends were observed in the degree of mineralization with the age of the fish, and significant variability was noted in the ^{44}Ca signals between individuals of the same or similar age which could not be accounted for by the inherent imprecision of the methodology. Kalish (1989) attributed this variability in salmon as within-individual differences in growth based on location, health, or somatic growth. Cailliet and Radtke (1987) also observed inter-annual variation in the magnitude and periodicity of the peaks and valleys of calcium and phosphorus with some individuals showing double peaks within a year, which they attributed to perturbations such as stress, changing temperature, or altered food availability. The variability in the calcium patterns in the round stingray may also be due to such perturbations, but further studies are necessary to resolve this issue.

Despite the observed intra- and inter-vertebrae variability in ion signals, reduced ion signals were consistently noted in the center of the structure and elevated ^{44}Ca signals were invariably observed from the edges of the structure when compared to the focus of the vertebrae. These findings are consistent with those of Cailliet and Radtke (1987) who also found a lower level of calcium and phosphorus in the vertebrae of the gray reef shark and the common thresher shark at the time of embryonic growth that was then followed by a peak in calcium and phosphorus at birth and first feeding. The focus of the vertebrae of the round stingray appears to have much lower levels of elements than the other parts of the vertebrae (other than barium, which appears to be enriched), but further analysis of this region is necessary to identify the natal signature of the round stingray. The elevated signals for ^{44}Ca at the outside edges of the vertebrae could be due to active calcification at the vertebrae perimeter (Cailliet and Radtke 1987). However, since all samples had an increase in analyte signal at the vertebrae edge irrespective of month captured, the elevated levels of elements could also be due to a topographical effect and the vertebral edge amplifying the efficiency of the ablation process (Reish and Mason 2003).

It is clear that LA-ICP-MS has great future potential for the elemental fingerprinting of elasmobranch cartilage. In particular, field and laboratory studies should be conducted to determine the degree of fidelity and distinctiveness of the elemental fingerprint to the chemistry of the surrounding environment. Round stingrays are seasonally abundant at Seal Beach (Hoisington and Lowe 2005) and Vaudo and Lowe (2006) found that these fish show seasonal site fidelity to this area. Additionally, the location of pupping for the round stingray is currently unknown, although it is thought to occur in inshore estuaries (Hoisington and Lowe 2005; Vaudo and Lowe 2006). Subtle changes in isotopic elemental signatures may provide a tool to track round stingray movements between estuarine and coastal habitats (Gillanders and Kingsford 2003; Gillanders 2005) and distinguish between genetically distinct populations of the round stingray in southern California (Campana et al. 1994, 2000; Thresher 1999; FitzGerald et al. 2004).

In conclusion, this preliminary study represents the first attempt to conduct spatial elemental analysis on the vertebrae of the round stingray. While the sensitivity of LA-ICP-MS is better than most other forms of microanalysis, the spatial resolution of the technique is inferior to both EDX and WDX. At present, the major limitation of the technique is that it is, at best, a semi-quantitative procedure (Durrant and Ward 2005).

Precision tends to be poor (5–8% under current conditions) even with short-wavelength, high energy lasers having high absorption efficiency and reduced ablation and plasma induced fractionation, and accurate quantification of elements in solid samples requires that the unknowns be carefully matrix-matched to certified standard reference materials (Durrant and Ward 2005). Consequently, accurate estimations of elemental content cannot be readily made by direct comparisons of signal intensities between different samples and this inherent limitation restricts the usefulness of the procedure to qualitatively study the relative distribution and content of elements within the sample (Durrant and Ward 2005).

Nevertheless, this technique appears to have potential for verifying age estimations and also quantify seasonal patterns in calcification. As suggested by Cailliet et al. (1986) and Cailliet and Radtke (1987), elemental microanalyses of growth bands lend credibility to age assessments derived from optical measurements. At the present time, the methods commonly used to assess the age of elasmobranchs are highly subjective (Goldman 2004). Optically-derived age estimates require the personnel be highly trained to ensure precision and decrease ageing errors and biases (Goldman 2004). Age assessment using LA-ICP-MS therefore provides an alternative, objective method to standard light microscopy for the verification of growth bands.

Acknowledgements Funding for field collections of stingrays was provided by University of Southern California Sea Grant Program, part of the National Sea Grant College Program, National Oceanic and Atmospheric Administration, U.S. Department of Commerce (Grant # NA86RG0054). Funding for the acquisition of the NewWave laser ablation system was provided by CSULB University College Extension. The GBC instrument was purchased by NSF MRI Grant# BCS 0321361. Funding for the analyses in this project was provided by CSUPERB. We would like to thank J. Neer for editorial comments, and J. Carlson and K. Goldman for the opportunity to publish these results with the proceedings of the symposia.

References

Andrews AH, Burton EJ, Kerr LA, Cailliet GM, Coale KH, Lundstrom CC, Brown TA (2005) Bomb radiocarbon and lead-radium disequilibria in otoliths of boccacio rockfish (*Sebastes paucispinis*): a determination of age and longevity for a difficult-to-age fish. Mar Freshwat Res 56:517–528

Cailliet GM, Radtke RL (1987) A progress report on the electron microprobe analysis technique for age determination and verification in elasmobranchs. In: Summerfelt RC, Hall GE (eds) The age and growth of fish. Iowa State University Press, Iowa, pp 359–369

Cailliet GM, Radtke RL, Weldon BA (1986) Elasmobranch age determination and verification: a review. In: Uyeno T, Arai R, Taniuchi T, Matsuura K (eds) Indo-Pacific fish biology: proceedings of the second international conference on Indo-Pacific fishes. Ichyol. Soc. Jpn., Tokyo, pp 385–360

Cailliet GM, Andrews AH, Burton EJ, Watters DL, Kline DE, Ferry-Graham LA (2001) Age determination and validation studies of marine fishes: do deep-dwellers live longer? Exp Gerontol 36:739–764

Campana SE (2005) Otolith science entering the 21st century. Mar Freshwat Res 56:485–495

Campana SE, Fowler AJ, Jones CM (1994) Otolith elemental fingerprinting for stock identification of Atlantic cod (*Gadus morhua*) using laser ablation ICP-MS. Can J Fish Aquat Sci 51:1942–1950

Campana SE, Thorrold SR, Jones CM, Gunther D, Tubrett M, Longerich H, Jackson S, Halden NM, Kalish JM, Piccoli P, de Pontual H, Troadec H, Panfili J, Secor DH, Severin KP, Sie SH, Thresher R, Teesdale WJ, Campbell JL (1997) Comparison of accuracy, precision, and sensitivity in elemental assays of fish otoliths using the electron microprobe, proton-induced X-ray emission, and laser ablation inductively coupled plasma mass spectrometry. Can J Fish Aquat Sci 54:2068–2079

Campana SE, Chouinard GA, Hanson JM, Frechet A, Brattey J (2000) Otolith elemental fingerprints as biological tracers of fish stocks. Fish Res 46:343–357

Campana SE, Natanson LJ, Myklevoll S (2002) Bomb dating and age determination of large pelagic sharks. Can J Fish Aquat Sci 59:450–455

Casselman J (1983) Age and growth assessments of fish from their calcified structures: techniques and tools. In: Prince E, Pulos L (eds) Proceedings of the international workshop on age determination of oceanic pelagic fishes: tunas, billfishes, and sharks. NOAA Tech. Rep. NMFS 8, pp 1–17

Durrant SF, Ward NI (2005) Recent biological and environmental applications of laser ablation inductively coupled plasma mass spectrometry (LA-ICP-MS). J Anal Atom Spectrom 20:821–829

FitzGerald JL, Thorrold SR, Bailey KM, Brown AL, Severin KP (2004) Elemental signatures in otoliths of larval walleye pollock (*Theragra chalcogramma*) from the northeast Pacific Ocean. Fish Bull 102:604–616

Gillanders BM (2005) Using elemental chemistry of fish otoliths to determine connectivity between estuarine and coastal habitats. Estuar Coast Shelf Sci 64:47–57

Gillanders BM, Kingsford MJ (2003) Spatial variation in elemental composition of otoliths of three species of fish (Family Sparidae). Estuar Coast Shelf Sci 57:1049–1064

Goldman KG (2004) Age and growth of elasmobranch fishes. In: Musick JA, Bonfil R (eds) Elasmobranch fisheries management techniques. APEC Fisheries Working Group, pp 97–132

Hale LF (2005) Age and growth of the round stingray, *Urobatis halleri*, at Seal Beach, California. MS Thesis, California State University Long Beach, p 42

Hoisington G, Lowe CG (2005) Abundance and distribution of the round stingray, *Urobatis halleri*, near a heated effluent outfall. Mar Environ Res 60(4):437–453

Jones BC, Geen GH (1977) Age determination of an elasmobranch (*Squalus acanthias*) by X-ray spectrometry. J Fish Res Board Canada 34:44–48

Kalish JM (1989) Otolith microchemistry: validation of the effects of physiology, age and environment on otolith composition. J Exp Mar Biol Ecol 132:151–178

Kastelle CR, Kimura DA, Jay SR (2000) Using $^{210}Pb/^{226}Ra$ disequilibrium to validate conventional ages in Scorpaenids (genera *Sebastes* and *Sebastolobus*). Fish Res 46:299–312

Leng MJ, Pearce NJG (1999) Seasonal variation of trace element and isotopic composition in the shell of a coastal mollusk, *Mactra isabelleana*. J Shellfish Res 18(2):569–574

Panfili J, Tomas J (2001) Validation of age estimation and back-calculation of fish length based on otoliths microstructures in tilapias (Pisces, Cichlidae). Fish Bull 99:139–150

Reish DJ, Mason AZ (2003) Radiocarbon dating and metal analyses of 'fossil' and living tubes of *Protula* (Annelida: Polychaeta). Hydrobiologia 496:371–383

Sanborn M, Telmer K (2003) The spatial resolution of LA-ICP-MS line scans across heterogeneous materials such as fish otoliths and zoned minerals. J Anal Atom Spectrom 18:1231–1237

Sinclair DJ, Kinsley LPJ, McCulloch MT (1998) High resolution analysis of trace elements in corals by laser ablation ICP-MS. Geochem Cosmochem Acta 62:1889–1901

Thresher RE (1999) Elemental composition of otoliths as a stock delineator in fishes. Fish Res 43:165–204

Trejos T, Montero S, Almirall JR (2002) Analysis and comparison of glass fragments by laser ablation inductively coupled plasma mass spectrometry (LA-ICP-MS) and ICP-MS. Anal Bioanal Chem 376(8):1255–1264

Vaudo J, Lowe CG (2006) Movement patterns of the round stingray, *Urobatis halleri* (Cooper), near a thermal outfall. J Fish Biol 68:1756–1766

Welden BA, Cailliet GM, Flegal AR (1987) Comparison of radiometric with vertebral band age estimates in four California elasmobranchs. In: Summerfelt RC, Hall GE (eds) The age and growth of fish. Iowa State University Press, Iowa, pp 301–315